Lawrence Berkeley National Laboratory
Recent Work

Title
ALPHA DECAY

Permalink
https://escholarship.org/uc/item/1495z8s1

Author
Mang, H.J.

Publication Date
1964-02-04

eScholarship.org Powered by the California Digital Library
University of California

UCRL-11326

# University of California

# Ernest O. Lawrence Radiation Laboratory

ALPHA DECAY

H. J. Mang

February 4, 1964

TWO-WEEK LOAN COPY

*This is a Library Circulating Copy which may be borrowed for two weeks. For a personal retention copy, call Tech. Info. Division, Ext. 5545*

Berkeley, California

## DISCLAIMER

This document was prepared as an account of work sponsored by the United States Government. While this document is believed to contain correct information, neither the United States Government nor any agency thereof, nor the Regents of the University of California, nor any of their employees, makes any warranty, express or implied, or assumes any legal responsibility for the accuracy, completeness, or usefulness of any information, apparatus, product, or process disclosed, or represents that its use would not infringe privately owned rights. Reference herein to any specific commercial product, process, or service by its trade name, trademark, manufacturer, or otherwise, does not necessarily constitute or imply its endorsement, recommendation, or favoring by the United States Government or any agency thereof, or the Regents of the University of California. The views and opinions of authors expressed herein do not necessarily state or reflect those of the United States Government or any agency thereof or the Regents of the University of California.

Submitted for publication in
Annual Review of Nuclear
Science

UCRL-11326

UNIVERSITY OF CALIFORNIA
Lawrence Radiation Laboratory
Berkeley, California

AEC Contract No. W-7405-eng-48

# ALPHA DECAY

H. J. Mang

February 4, 1964

# ALPHA DECAY

H. J. Mang

Lawrence Radiation Laboratory
University of California
Berkeley, California

February 4, 1964

## I. Introduction

Alpha radioactivity has long been a valuable tool of the nuclear spectroscopist, and in recent years has yielded an ever increasing amount of energy-level information. The monoenergetic character of $\alpha$ radiation (like $\gamma$ radiation) and its charged-particle nature (like $\beta$ radiation) make possible precision spectroscopy by large magnetic spectrographs down to line widths of a few keV. Lower-resolution spectroscopy, but with high geometry, is performed often with ionization chambers and solid-state semiconductor detectors.

Alpha transitions, in contrast to $\beta$ and $\gamma$ transitions, are only mildly inhibited by changes in angular momentum. Therefore, all the low-lying states of the daughter nucleus are likely to be populated in detectable intensity. As a spectroscopic tool, $\alpha$ radiation suffers from two restrictions. First, it is limited to certain regions of the periodic table, the largest encompassing the trans-lead nuclei, and another consisting of rare earth nuclei with 84 or a few more neutrons. The second restriction is that $\alpha$-transition rates exhibit an extremely sensitive dependence on decay energy, so that in practice only states up to a few hundred kilovolts excitation are populated in $\alpha$ decay.

In the trans-lead region, where $\alpha$ decay is so prevalent, the Q values of $\alpha$ and $\beta$ decay have been used to calculate relative atomic

masses within the four connected families whose mass numbers are of form $4n$, $4n+1$, $4n+2$, and $4n+3$. When supplemented by three nuclear reaction Q values, the families are linked together to give atomic masses over the whole heavy region (1,2). Besides the importance of energy measurements, $\alpha$ decay rates--and particularly the fine-structure patterns (3)--are interesting in their own right.

The dominating factor governing $\alpha$ decay rates has long been recognized as the Coulombic barrier penetration. Indeed it was one of the triumphs of quantum mechanics when Gamow (4) and, independently, Condon & Gurney (5) were able to show that this barrier-penetration factor and its energy dependence follow from the quantum mechanical treatment of a simple model of $\alpha$ decay. In this model the $\alpha$ emitter is treated as an $\alpha$ particle moving in a potential well supposedly created by the remaining nucleons.

Clearly such a one-body model is not sophisticated enough to allow an understanding of the relation of the fine-structure pattern to nuclear structure. A first attempt was made by R. G. Thomas in 1954 to treat $\alpha$ decay as a many-body problem (6). His approach to the problem is based on the R-Matrix theory of Wigner & Eisenbud (7). He did not pursue his approach further, however; in particular, he did not use nuclear-model wave functions to calculate $\alpha$-transition rates.

The development in recent years has been going exactly in this direction (8-12), and the more subtle connections of $\alpha$ decay with the powerful concept of the nuclear shell model are becoming more and more clear. Certainly a complete understanding of this relation will enable us to obtain further and more detailed information about energy levels, from $\alpha$ decay measurements.

For this very reason this article is almost entirely devoted to the problem of $\alpha$ decay rates and nuclear models.

## II. Conservation Laws and Basic Equations

The $\alpha$ decay process for bare nuclei has the equation

$$(Z + 2)^{A+4} \longrightarrow Z^{A} + {}_{2}He^{4} \quad .$$

Conservation of energy requires that at infinitely large separation of the products, the effective kinetic energy $Q_f$ of the final system be given by the difference of rest masses of the nuclei times the square of the velocity of light,

$$Q_f = (M_{A+4} - M_A - M_{He})\, c^2 \quad .$$

The Q values for nuclear $\alpha$ decay rarely exceed 0.25% of the reduced mass, $M_\alpha$ ( $= \frac{M_{He} \times M_A}{M_{He} + M_A}$ ). Hence, nonrelativistic treatments may be confidently employed.

Conservation of linear momentum then requires that the total kinetic energy be divided between the two products in inverse proportion to their masses.

The quantity $Q_f$ is desired for careful theoretical treatment of $\alpha$ decay rates, but the Q value that can be directly measured in the laboratory is somewhat different, since one actually deals with atoms possessing a cloud of orbital electrons. The simple two-body breakup expressed by the equations above is an idealization to be inferred from a many-body problem with the electrons in the system. Because the electrons are so much

lighter than the nuclear bodies, their presence does not usually make for difficulties in inferring properties of the decay process of the bare nuclei. The $Q_f$ value may be obtained from the measured $Q$ value by adding the "Screening correction" (13),

$$\Delta E_{SC} = 65.3\, Z^{7/2} - 80\, Z^{2/3} \text{ev},$$

where $Z$ is the atomic number of the parent.

In applying the laws of conservation of angular momentum and parity it is appropriate again to consider the two-body breakup of the bare nuclei and neglect the orbital electrons. The electrons make their presence felt only in attenuating angular correlations, essentially breaking down the conservation of the projection of nuclear angular momentum along a space-fixed axis (14).

The parity, and the total angular momentum and its projection along an axis, should be the same for the final system as for the initial parent nucleus. Since the $\alpha$ particle is spinless and has even parity, the selection rules take an especially simple form. The orbital angular momentum of $\alpha$ decay is restricted to values between the sum and difference of initial and final spins,

$$|I_i - I_f| \leq L \leq I_i + I_f \ .$$

If the parity of parent and daughter are the same, only even values of L are permitted; if oposite, then only odd values of $L$ are permitted. The conservation of the projection of angular momentum may be expressed in terms of the magnetic quantum numbers. This conservation is relevant to angular correlation experiments.

If parent (or daughter) has spin zero, than certain spin and parity combinations of the daughter (or parent) states will be absolutely forbidden to the extent that parity is conserved in strong interactions. The orbital electrons could, of course, mix in certain states, which woulc cause a biolation of the selection rule. The magnitude of the amplitudes of such admixtures, however, would be given by the ratio of magnetic hyperfine splitting to the energy separation of the admixed nuclear states.

A formula that expresses the decay constant in terms of nuclear wave functions is now derived. The derivation is based on the assumption that (a) the decaying system can be described by a wave function $\Phi_J^M (X_1 \cdots X_A; t)$ which depends on A space and spin coordinates $X_k (k = 1 \cdots A)$ and the time t; and moreover, (b) that we know the functional form of the time dependence within a certain space-time region (15).

Let $\chi_\alpha$ be the internal $\alpha$-particle wave function, and $\psi_{jJ}^m$ a set of wave functions of the daughter nucleus.

We define

$$g^J_{j\ell}(R,t) = \left[\binom{N}{2}\binom{Z}{2}\right]^{1/2} \int \sum_m C(\ell j J; m\ M-m) \times Y_\ell^m(\theta,\psi)\, \psi_j^{M-m}(\eta)\, \chi_\alpha(\xi)\, \Phi_J^{*M}(x_1 \cdots x_A, t)\, d\xi\, d\eta\, d\Omega, \qquad \text{II.1}$$

where

R = relative distance between $\alpha$ particle and daughter nucleus,

$\Omega = (\theta,\psi)$ = angular coordinates of the $\alpha$ particle with respect to the center-of-mass system,

$\xi$ = internal coordinates of the $\alpha$ particle

$\eta$ = internal coordinates of the daughter nucleus,

$\xi$ and $\eta$ stand for space and spin coordinates,

$J$ = total angular momentum of the parent nucleus,

$j$ = total angular momentum of the daughter nucleus,

$\ell$ = angular momentum of the $\alpha$ particle relative to the daughter nucleus,

$M$, $m$ = magnetic quantum numbers,

$C(\ell j J; m\ M-m)$ = Clebsch-Gordan coefficient

Here $\binom{N}{2}$ and $\binom{Z}{2}$ are binomial coefficients which account for the fact that the final-state wave function ($\alpha$ + daughter) has not been completely anti-symmetrized. Clearly $g^J_{j,\ell}(R,t)$ has the meaning of a time-dependent probability amplitude. It measures the probability that in the wave function $\phi^M_J$ an $\alpha$ particle and a daughter nucleus with the specified quantum numbers are present at a distance $R$ of each other and at a time $T$. It should be mentioned that angular momentum conservation has been taken into account explicitly by coupling the angular momenta of the $\alpha$ particle, $\ell$, and daughter nucleus, $j$, to give the angular momentum of the parent nucleus, $J$. Furthermore, to aviod too many indices, all quantum numbers necessary to specify a nuclear state are considered to be included in the angular momentum quantum numbers $j,J$.

The conditions for $\phi^M_J$ to describe a proper decaying state are as follows:

(a) There exists a space-time region in which the time dependence of $g^J_{j,\ell}(R,t)$ is exponential,

$$g^J_{j,\ell}(R,t) = \exp\left[\frac{-i}{\hbar}(E-i\Gamma)t\right] g^J_{j,\ell}(R), \qquad \text{II.2}$$

with $E$ and $\Gamma$ real and $\Gamma$ also positive,

(b) For sufficiently large distances $R$ the amplitude $g^J_{j,\ell}(R)$ may contain only outgoing waves.

The restrictions on the space-time region in which the above conditions can be fulfilled are evident. Equation II.2 can never hold for all times t. Clearly it cannot hold for sufficiently large negative times t. Indeed the decaying system must have been formed at some time, and it does not make sense to apply Equation II.2 to any time prior to that formation. Also, Equation II.2 is not valid for very large positive times. This is because of the dispersion of a wave packet leading to a time dependence like $t^{-3/2}$, which finally dominates over any exponential time dependence. The space region in which the above conditions can be fulfilled is also limited. Suppose the decaying system has been formed at a time $t_o = 0$, then at time $t$ and $\alpha$ particle can have traveled only a distance $R = vt$ ($v$ = velocity of the $\alpha$ particle). It follows that for $R > vt$ the amplitude $g^J_j(R,t)$ must be essentially zero. It has been shown, however, that these restrictions are unimportant in all practical cases (16, 17). There is always a sufficiently large space-time region in which conditions (a) and (b) can be fulfilled with an extremely high degree of precision.

Starting from Equation II.2 it is easy to express the decay constant $\lambda$ in terms of the amplitudes $g^J_{j,\ell}(R)$. One obtains, from the continuity equation,

$$\lambda = \frac{2\Gamma}{\hbar} = \sum_{j,\ell} \lambda^J_{j,\ell}, \qquad \text{II.3}$$

with

$$\mathfrak{J}^J_{j,\ell} = \frac{R^2}{2iM}\left[g^{*J}_{j\ell}\cdot\frac{}{R}\,g^J_{j\ell} - g^J_{j\ell}\cdot\frac{}{R}\,g^{*J}_{j\ell}\right], \qquad \text{II.4}$$

where M = reduced mass of the $\alpha$ particle.

In the region of R larger than vt, where the asymptotic form of the amplitudes $g^J_{j\ell}$ can be used, Equation II.4 reduces to

$$\mathfrak{J}^J_{j\ell} = v \cdot R^2 \left|g^J_{j\ell}(R)\right|^2 . \qquad \text{II.5}$$

At this point it should be noted that in going from Equation II.4 to Equation II.5, use has been made of the fact that there is a sufficiently large space-time region in which Equation II.2 may be applied. Indeed, the time t must be so large that the point R = vt is well within the asymptotic region where $g^J_{j\ell}(R)$ behaves like a simple outgoing wave and $R^2\left|g^J_{j\ell}(R)\right|^2$ is therefore independent of R. Finally, the crucial approximation must be introduced, which will allow the calculation of the amplitudes $g^J_{j\ell}(R)$ from nuclear models.

Assume the existence of a radius $R_0$ so that (8, 15):

(c) For $R > R_0$ the interaction between $\alpha$ particle and daughter nucleus can be represented by a potential V(R) alone.

(d) For $R < R_0$ nuclear-model wave functions allow a calculation of the amplitudes $g^J_{j\ell}$. Each condition can be individually fulfilled--condition (c) by choice of a sufficiently large $R_0$, and (d) with the help of a radius $R_0$ that is small enough. Whether a satisfactory compromise is possible will finally be decided by success or failure of a theory based on the existence of such a radius $R_0$. One can write $g^J_{j\ell}(R)$ as

$$g^J_{j\ell}(R) = g^J_{j\ell}(R_0)\ \frac{g^J_{j\ell}(R)}{g^J_{j\ell}(R_0)} \quad . \qquad \text{II.6}$$

According to condition (c) the ratio $g^J_{j\ell}(R)/g^J_{j\ell}(R_0)$ is calculable from a one-body Schrödinger equation. Into the solution enters the potential V(R) and the asymptotic boundary condition that there are only outgoing waves. The WKB approximation (18), which has been almost exclusively used in α-decay theory, yields a simple expression

$$\left|\frac{Rg^J_{j\ell}(R)}{R_0 g^J_{j\ell}(R_0)}\right|^2 = \frac{q(R_0)}{k}\ \exp\left[-2\int_{R_0}^{r_0} q(r)\,dr\right], \qquad \text{II.7}$$

where

$$q(r) = \left\{\frac{2M}{\hbar^2}\left[\epsilon - \frac{\hbar^2}{2M}\ \frac{(\ell+1/2)^2}{r^2} - V(r)\right]\right\}^{1/2},$$

$\epsilon$ = kinetic energy of the α particle,

$k = \frac{2M}{\hbar^2}\epsilon$,

and $r_0$ = outer turning point defined by $q(r_0) = 0$.

Next $\lambda$ is expressed in terms of barrier penetrability $P_\ell(\epsilon)$ and reduced width $\gamma^2_{Jj\ell}$:

$$\lambda = \frac{1}{\hbar}\sum_{j\ell} P_\ell(\epsilon)\ \gamma^2_{Jj\ell} \qquad \text{II.8}$$

The definitions are

$$\gamma^2_{Jj\ell} = \frac{\hbar^2}{2M} R_0 |g^J_{j\ell}(R_0)|^2 \qquad \text{II.9}$$

$$= \frac{\hbar^2}{2MR_0^2} \left| G^J_{j\ell}(R_0) \right|^2$$

with

$$G^J_{j\ell}(R_0) = R_0^{3/2}\, g^J_{j\ell}(R_0),$$

and

$$P_\ell(\epsilon) = 2kR_0 \left| \frac{R\, g^J_{j\ell}(R)}{R_0\, g^J_{j\ell}(R_0)} \right|^2 = 2R_0 q \exp\left(-2\int_{R_0}^{r_0} q\,(r)\, dr\right)$$

The $G^J_{j\ell}(R_0)$ is now a dimensionless quantity. Clearly both $P_\ell(\epsilon)$ and $\gamma^2_{Jj\ell}$ depend on $R_0$, but their product should be independent of $R_0$ in an exact theory. This point is discussed in detail in references 11 and 15.

The amplitude $G^J_{j\ell}(R_0)$ can now be calculated from Equation II.1, in which $\Phi^M_J$, the wave function of the decaying system, may be replaced by the wave function of the parent nucleus in accordance with the choice of the radius $R_0$:

$$G^J_{j\ell}(R_0) = R_0^{3/2} \left[ \binom{N}{2} \binom{Z}{2} \right]^{1/2} \int \sum_m C(\ell j J;\, m\ M-m)$$

$$\times Y^m_\ell\,(\theta\psi)\ \Psi^{M-m}_j\,(\eta)\ \chi_\alpha(\xi)\ \Phi^M_J\, d\xi\, d\eta\, d\Omega \quad . \qquad \text{II.10}$$

The content of this chapter can be summarized as follows: The $\alpha$-decay constant can be expressed as a sum of partial transition probabilities (the sum on $j,\ell$). More important, however, the partial transition probabilities consist of two factors, one representing the probability of formation of an $\alpha$-particle in the nuclear surface region $^2_{Jj\ell}(R_0)$, the other measuring the probability of penetration through the Coulomb barrier. The problem of calculating the decay constant has been divided into two

problems, one of which, the calculation of $\gamma^2_{Jj\ell}$, involves specific nuclear properties of the parent and daughter nucleus, whereas the barrier penetrability depends only on the decay energy and the α-nucleus potential V(R) whose main part, the Coulomb potential $\frac{2Z\,e^2}{R}$, is well known. The second problem has been recognized and solved by Gamow (4), and also by Condon & Gurney (5). The barrier penetrability $P_\ell\,(\epsilon)$ determines the the extremely strong exponential energy dependence of the decay constant. A thorough discussion of this point can be found in reference 13. We shall from now on concentrate on the reduced width $\gamma^2_{Jj\ell}$ that contains all the information on nuclear properties.

## III. Spherical Nuclei

In the preceding chapter the assumption has been made that the α-nucleus interaction consists of a simple potential V(R) as long as α particle and daughter nucleus are farther apart than $R_0$. This implies that there is no interaction leading to excitation or de-excitation of the daughter nucleus by the α particle while it penetrates the barrier. Such an asumption can be valid only if the nuclei involved in the decay have spherical equilibrium shape.

Furthermore we shall want to invoke the nuclear shell model in the explanation of α-decay data, since it is a simple model of nuclear structure. Therefore it seems only natural to concentrate first on the region in the periodic table around doubly magic $Pb^{208}$. If shell-model wave functions have anything to do with reality, then nuclear wave functions in this region whould be reasonably well approximated by them.

Before the implications of the nuclear shell model for the α-decay process can be discussed, the question of the internal α-wave function $\chi_\alpha(\xi)$ must be settled. Electron scattering experiments on He (19) are explained by a charge density distribution of Gaussian shape. This leads to a wave function of the type

$$\chi_\alpha(\xi_1\xi_2\xi_3 s_1 s_2 s_3 s_4) = \chi_0^0(s_1 s_2)\, \chi_0^0(s_3 s_4) \left( \frac{2\beta^{3/2}}{\frac{1}{2}!\, 4\pi} \right)^{3/2} \exp\left[ -\frac{\beta}{2} (\xi_1^2 + \xi_2^2 + \xi_3^2) \right] , \qquad \text{III.1}$$

where

$$\underset{\sim}{\xi}_1 = (1/\sqrt{2}) \ (\underset{\sim}{r}_1 - \underset{\sim}{r}_2) \ ,$$

$$\underset{\sim}{\xi}_2 = (1/\sqrt{2}) \ (\underset{\sim}{r}_3 - \underset{\sim}{r}_4) \ ,$$

$$\underset{\sim}{\xi}_3 = (1/2) \ (\underset{\sim}{r}_1 + \underset{\sim}{r}_2 + \underset{\sim}{r}_3 + \underset{\sim}{r}_4) \ ,$$

$s_1$, $s_2$, $s_3$, $s_4$ = spin coordinates,

$\chi_0^0$ = singlet spin function,

1,2 refer to protons,

3,4 refer to neutrons,

and $\beta = 0.47 \cdot F^{-2}$ .

The above wave function will be used throughout. It should be noted at this point that the following relation between volume elements holds:

$$d^3r_1\, d^3r_2\, d^3r_3\, d^3r_4 = 8\, d^3\xi_1\, d^3\xi_2\, d^3\xi_3\, d^3R.$$

All wave functions in the following are normalized with the volume element $d^3\xi_1\, d^3\xi_2\, d^3\xi_3\, d^3R$.

An interesting set of data to be studied first is the decay properties of the even-even polonium isotopes. The ground-state transitions ($0^+ \rightarrow 0^+$) are always the most intense transitions. Transitions to excited states are considerably hindered owing to the energy and angular momentum dependence of the barrier penetrability. Lifetimes and decay energies are known for all mass numbers from A = 202 to A = 220 (13, 20). Assuming a potential V(R) for the $\alpha$-nucleus interaction, one can calculate the reduced widths. Two sets of such reduced widths are plotted against the mass number in Fig. 1. These two sets of reduced widths are given in an attempt to demonstrate that the general behavior of the reduced width as a function of the mass number is not altered when the potential is somewhat changed. The potentials used were a pure Coulomb potential ($R_0$ = 9.3 F) and the real part of Igo's optical-model potential (21,22) which has been derived from scattering data.

It is almost unnecessary to point out the conspicuous increase of the reduced width when going from A = 210 to A = 212 (or from neutron number 126 to 128). Such an increase can be understood qualitatively from the structure of the formula for the reduced width (Equation II.9). On the basis of the shell model the the nucleus $Po^{212}$ differs from $Pb^{208}$ by two neutrons and two protons outside the closed shells, whereas $Po^{210}$ has only two protons outside the closed shells. In order to form the daughter nucleus $Pb^{206}$ in the latter case the closed neutron shell must be broken. In this picture the probability amplitude for formation of an $\alpha$ particle is directly related to the magnitude of the single-particle

wave functions at the nuclear surface. That this is so can be seen from Equation II.10. After integration over the internal coordinates of the daughter nucleus is performed, a wave function of four nucleons is left. From this four-nucleon wave function an $\alpha$ particle with its center of mass at $R_0$ contribute. According to the shell model the four-nucleon wave functions involved are the same in both decays. The neutron wave functions, however, belong to different single-particle states. Since the single-particle states that form the closed shell are more strongly bound than the ones outside the closed shell, it is to be expected that the wave functions corresponding to the latter are larger at the edge of the nucleus. Therefore, the reduced width of $Po^{212}$ should be larger than the reduced width of $Po^{210}$. That this explanation is correct shows in a calculation in which the single-particle wave functions have been approximated by harmonic oscillator wave functions (9). The order in which the various single-particle states are filled or emptied has been determined with the help of the energy levels of nuclei which have one nucleon more or less than $Pb^{206}$. These are $Pb^{207}$, $Tl^{207}$, $Pb^{209}$, and $Bi^{209}$. Their level schemes are given in Table I; they are important to what follows. The calculated values in Fig. 2 are all given relative to the standard $Po^{210}$. The reason for doing this is that ratios of reduced widths are insensitive to parameter changes. For instance, $R_0$ can be varied between 8.0 and 9.5 F and the ratios of reduced widths remain practically unchanged. The absolute values, however, are extremely sensitive to such changes. This question will be taken up later.

The comparison between experimental and calculated reduced width in Fig. 2 shows very clearly that taking into account nuclear structure effects on the basis of a simple shell model improves markedly the

agreement between experiment and theory. It is no longer necessary to invoke a discontinuous change in nuclear radius when going from $Pb^{206}$ to doubly magic $Pb^{208}$. Indeed such a radius change has never been supported by any other experiment.

A natural question to ask is what happens if refinements of the shell model are brought into the picture. Is the agreement between experiment and theory improved or wiped out altogether?

In order to answer such questions four particularly suitable decays have been studied in great detail (10, 12). The parent nuclei were $Po^{210}$, $Po^{211}$, $Po^{212}$, and $Bi^{211}$. The shell model has been refined in two respects. First, configuration mixing was introduced (23, 24), and second, the harmonic oscillator wave functions were replaced by wave functions calculated with the help of a single-particle potential of the Woods-Saxon type (25). The results of the calculation as well as the experimental values of the decay amplitudes are presented in Table II. It should be noted that the experimental data are complete in the sense that practically all possible measurements have been performed (26-29), including an $\alpha$-$\gamma$ polarization correlation measurement in the decay of $Bi^{211}$ to the first excited state of $Tl^{207}$ (29). This experiment together with an $\alpha$-$\gamma$ angular correlation measurement (27) determines the relative amplitude of the $\alpha$ partial waves and the multipole mixture of the subsequent $\gamma$ transition. One can but conclude that the more sophisticated the model the better the agreement between experiment and calculation. We must admit, however, that the almost perfect agreement of the last two columns in Table II may well be accidental.

The transitions discussed so far are not the only ones in the region around $Pb^{208}$ that are well studied. Some odd-odd $\alpha$ emitters such

as $Bi^{210}$ and $Bi^{212}$ show a very complex fine structure (30, 31), and some isomeric states such as $Bi^{210}$ isom, $Po^{211}$ isom, and $^{212}$ isom are of interest because of these extreme spin values (27, 32-35). The spins and parities assigned to these states are 9-, $\frac{25}{2}$ +, and 18 +. Only the assignment of the $Bi^{210}$ isomer has been confirmed by another experiment, the (d,p) reaction on $Bi^{209}$; the two others are based on α-decay data alone. These α transition are not very helpful in supporting the shell-model theory of α decay. There is no reason to believe that the wave functions are pure shell-model wave functions (36, 37), and admixtures to shell-model wave functions can be shown to be important (12). With some confidence in the theory, however, one could attempt to investigate these wave functions with the help of α-decay studies.

## IV. The BCS Method and Alpha Decay Rates

The results so far obtained on the basis of a refined nuclear shell model are certainly encouraging enough to justify an attempt to apply the theory to many more α emitters. For nuclei far removed from closed shells, however, the simple shell model is not adequate and configuration mixing calculations are not feasible. Fortunately the Bardeen-Cooper-Schrieffer Method (38, 39), borrowed from the theory of superconductivity and sucessfully applied to nuclear physics (40-44), allows one to account for the most important correlations between nucleons outside closed shells in a reasonably good approximation. It goes beyond the scope of this article to develop the BCS theory or to justify its use in nuclear structure calculations. Only the results can be presented.

The nuclear wave function is written as a product of a neutron wave function and a proton wave function:

$$\Phi = \Psi(\text{protons}) \times \Psi(\text{neutrons}) \qquad \text{IV.1}$$

with

$$\Psi = \prod_{\Omega} (U_\Omega + V_\Omega \, b_\Omega^+ \, b_{-\Omega}^+)|0\rangle \qquad \text{IV.2}$$

for an even system,

or

$$\Psi = b_k^+ \prod_{\Omega \neq k} (U_\Omega + V_\Omega \, b_\Omega^+ \, b_{-\Omega}^+)|0\rangle \qquad \text{IV.3}$$

for an odd system.

$$U_\Omega^2 + V_\Omega^2 = 1 \quad . \qquad \text{IV.4}$$

The index $\Omega$ labels the single-particle states. The state $\Omega$ is the time-reversed state of $\Omega$. When dealing with a spherical nucleus, $\Omega$ stands for the set of quantum numbers $(n \; \ell \; j \; m)$. In this particular case the amplitudes $V_\Omega$ and $U_\Omega$ are also independent of the magnetic quantum number m. This corresponds to coupling like nucleons pairwise to angular momentum zero. In the general case the states $\Omega$ may form any set of single particle states. The quantities $V_\Omega$ and $U_\Omega$ are probability amplitudes where $V_\Omega^2$ measures the probability for the state $\Omega$, $-\Omega$ being occupied by a pair of nucleons whereas $U_\Omega^2$ measures the probability that this state is unoccupied. Equations to determine $U_\Omega$ and $V_\Omega$ are obtained by minimizing the expectation value of the Hamiltonian. Usually $U_\Omega$ and $V_\Omega$ are then expressed in terms of the chemical potential $\lambda$, the gap parameters $\Delta\Omega$ and the single-particle energies $\epsilon\Omega$ ,

$$V_\Omega^2 = (1/2) \left[ 1 - (\epsilon_\Omega - \lambda)/\sqrt{(\epsilon_\Omega - \lambda)^2 + \Delta_\Omega^2} \right]$$

$$U_\Omega^2 = (1/2) \left[ 1 + (\epsilon_\Omega - \lambda)/\sqrt{(\epsilon_\Omega - \lambda)^2 + \Delta_\Omega^2} \right] \qquad \text{IV.5}$$

Clearly the states with single-particle energies smaller than $\lambda$ are more than half filled ($V_\Omega^2 > 0.5$) and the others less than half filled ($V_\Omega^2 < 0.5$). The gap parameters $\Delta_\Omega$ measure the diffuseness of the "probability distribution" ($V_\Omega^2$), where the amplitudes $V_\Omega$ are considered as functions of the single-particle energy. In other words, $\Delta_\Omega$ measures the deviation of the function $V_\Omega(\epsilon)$ from a step function, since for $\Delta_\Omega$ tending towards zero the occupation probabilities $V_\Omega^2$ are either one or zero depending on the position of the corresponding single-particle energy $\epsilon_\Omega$ relative to the chemical potential $\lambda$.

Upon introducing the wave function IV.1 into Equation II.10 the quantity $G^J_{j\ell}(R_0)$--and hence the reduced width--is obtained in terms of the amplitudes $U_\Omega$, $V_\Omega$.

As a first example, the ground-state transitions of even-even nuclei are considered (in this case $J = j = \ell = 0$):

$$G^0_{00}(R_0) = \sum_{j_p j_N} \prod_{j_p'} \left(U^i_{j_p'} U^f_{j_p'} + V^i_{j_p'} V^f_{j_p'}\right) \left(2j_{p'}+1/2 - \delta_{j_p j_{p'}}\right)$$

$$\times \prod_{j_N'} \left(U^i_{j_N'} U^f_{j_N'} + V^i_{j_N'} V^f_{j_N'}\right) \left(2j_{N'}+1/2 - \delta_{j_N j_{N'}}\right) \qquad \text{IV.6}$$

$$\times \ (1/2) \left[(2j_p+1)\ (2j_N+1)\right]^{1/2} U^f_{j_p} V^i_{j_p} U^f_{j_N} V^i_{j_N} \Gamma^{(0)}_{j_p j_p 0 j_N j_N 00}(R_0),$$

with

$$\Gamma^{(0)}_{j_1 j_2 J_p j_3 j_4 J_N L} = \sum_{\substack{m_1 m_3 \\ M_p M_N}} C(j_1 j_2 J_p;\ m_1\ M_p - m_1)$$

$$\times\ C(j_3 j_4 J_N; m_3\ M_N - m_3)\ C(J_p J_N L; M_p M_N)$$

$$\times R_0^{3/2} \int \chi_\alpha^*(\xi_\alpha)\, Y_L^{M*}(\Omega)\; A\left(\psi_{j_1}^{m_1}\psi_{j_2}^{M_p-m_1}\right)\; A\left(\psi_{j_3}^{m_3}\psi_{j_4}^{M_N-m_3}\right) d\xi_\alpha d\Omega, \quad (IV.6)$$

where $\psi_j^m$ = single-particle wave function of the state $n\ell jm$ (the quantum numbers $n$ and $\ell$ are not explicitly written),

and $A$ = antisymmetrization and normalization operator.

The quantity $\Gamma$ is the amplitude for $\alpha$ formation from four nucleons in single-particle states $j_1 j_2 j_3 j_4$ where the protons $(j_1 j_2)$ are coupled to $J_p$ and the neutrons $(j_3 j_4)$ are coupled to $J_N$. In the above example all angular momenta are zero $(j_n = J_p = L = 0)$ because of the special coupling of the single particles in the initial and final nucleus.

The factor $J_j^f V_j^i$ is easily understood. In the $\alpha$-decay process a pair of nucleons is taken away from the parent nucleus. If the pair is to be taken from the state $j$ this state must be occupied in the parent nucleus, hence the amplitude $V_j^i$ appears, and when the pair has been removed the state must be unoccupied in the daughter nucleus, therefore the factor $U_j^f$ must be present in Equation IV.6.

The expressions which apply to odd-mass nuclei or to excited-state transitions in even-even nuclei are slightly more complicated and are not given here. They can be found in reference 15. Equation IV.6 has been used by Zeh (15) and also by MacFarlane, Rasmussen & Rho (45) to calculate reduced widths of even-even spherical nuclei. Zeh has treated once again the even-mass isotopes of polonium and finds no drastic difference from a calculation based on the simple shell model (9), except for the absolute value of the reduced width, which increases by a factor of ten. He points out that fluctuations related to the existence of subshells are reduced when pairing correlations are included in the shell-model calculation. MacFarlane et al. discuss the decays of rare

earth $\alpha$ emitters which have neutron number $N = 84$ (46-48). They are able to explain the variation of the reduced width with proton number Z, but only if they choose the proper single-particle energies for the proton states and a suitable strength of the pairing interaction. It is worth mentioning that although there is a close analogy between the neutrons in the rare earth $\alpha$ emitters $N = 84$ and the protons in the polonium case ($Z = 84$) the situation is quite different for the other type of nucleons in the two cases. The rare earth $\alpha$ emitters have always an appreciable number of protons outside closed shells, since Z ranges from 58 to 70. In evaluating the importance of pairing correlations for the $\alpha$-decay problem from these examples one should keep in mind that in the j-j coupling shell model (49) one has included pairing correlations between nucleons in one subshell (same j). What the BCS treatment adds are correlations between nucleons in different subshells (different j). The situation is radically different in the case of deformed nuclei, in which all levels are only twofold degenerate. There pairing correlations are decisive.

## V. Deformed Nuclei

The treatment of deformed nuclei is based on two assumptions concerning the nuclear wave functions.

First, the validity of the strong coupling model of Bohr and Mottelson (50) is taken as granted. This implies that the total nuclear wave function factorizes into a rotational and an intrinsic part:

$$\Phi_I^{MKq} = (2I+1/16\pi^2)^{1/2} \left[ D^I_{MK}(\theta_i)\, \Phi_k + (-1)^{I-K+q} D^I_{M-K}(\theta_i)\, \Phi_{-K} \right] \qquad \text{V.1}$$

where

I = total angular momentum,

M = magnetic quantum number,

K = projection of the total angular momentum on the nuclear symmetry axis,

and $(-1)^q$ = parity.

The functions $D^I_{MK}$ are the eigenfunctions of a symmetric top. The arguments $\theta_i$ are the Eulerian angles which connect the "body fixed" nuclear coordinate system with a "space fixed" frame of reference. The wave functions $\phi_K$ describe the intrinsic motion of the nucleons with respect to the "body fixed" coordinate system.

The second assumption concerns these intrinsic wave functions. They are of the BCS type, with single-particle wave functions calculated from a deformed average potential. The single-particle wave functions used in the following are taken from Nilsson's work (51, 52).

A complication stems from the large intrinsic quadrupole moments in the deformed region. The quadrupole moment of the daughter nucleus leads to a

coupling between different final states which cannot be neglected as was done in the case of spherical nuclei. When the $\alpha$ particle penetrates the nuclear barrier it may well exchange energy and angular momentum with the daughter nucleus.

The states of the daughter nucleus that are involved in this process are the members of a rotational band, exactly those states that are connected by strong electric quadrupole transitions. In other words, to calculate the barrier penetrability one no longer deals with a simple one-dimensional Schrödinger equation as in the spherical case, but either with a three-dimensional Schrödinger equation that is not separable or with a set of coupled differential equations for the radial wave functions in the case in which the $\alpha$ wave function is expanded in spherical harmonics. The barrier penetrability $P_\ell(\epsilon_j)$ has to be replaced by a penetrability matrix $Q_{\ell j}^{Im}$, which accounts for the possibility that an $\alpha$ particle formed with angular momentum L and magnetic momentum $\ell$, leaving the daughter nucleus in a rotational state j. The penetrability matrix is conventionally written as a product of two factors. The square of the first factor is the usual barrier penetrability calculated as in the spherical case. The second factor, $B_{\ell j}^{Im}$, takes the matrix character. It should be emphasized that this is mere convention. What has just been said can be restated by saying that Equation II.6 is/now a matrix equation. This equation connects the asymptotic flux with the $\alpha$ amplitude at the nuclear surface. Proceeding exactly as in Chapter II, one can thus obtain an expression for the partial transition probability from a state $I_i\ k_i\ q_i$ of the parent to a state $I_f\ k_f\ q_f$ of the daughter by emission of an $\alpha$ particle with angular momentum $\ell$:

$$\lambda_{I_f K_f q_f \ell}^{I_i K_i q_i} = \frac{1}{\hbar} P_\ell(\epsilon_{I_f}) \frac{2}{2MR_0^2} \left| \sum_L B_{\ell I_f}^{L K_i - K_f} G_{L K_i - K_f}^{(R)} \right.$$

$$\left. + (-1)^{I_i - L - K_f} B_{\ell I_f}^{L K_i + K_f} G_{L K_i + K_f}^{(R)} \right|_{R = R_0}^2 \qquad \text{V.2}$$

The functions $G_{L\,K_i-K_f}$ and $G_{L\,K_i+K_f}$ again are the α-probability amplitudes at the nuclear surface ($R = R_0$). The presence of two terms is due to the two terms $(\Phi_K, \Phi_{-K})$ in the strong-coupling wave function. The α particle at the nuclear surface may take either the difference or the sum of the projection quantum numbers $K_i$ and $K_f$. A reduced width can be defined as in the case of a spherical α emitter.

$$G_{L\,K_i-K_f} = R^{3/2}\left[\binom{N}{2}\binom{N}{2}\right]^{1/2}\int \Phi^*_{K_i}\,\chi_\alpha\,\Phi_{K_f}\,Y_L^{K_i-K_f}(\Omega')\,d\xi\,d\eta\,d\Omega' \,,$$

$$G_{L\,K_i+K_f} = R^{3/2}\left[\binom{N}{2}\binom{N}{2}\right]^{1/2}(-1)^{q_f}\int \Phi^*_{K_i}\,\chi_\alpha\,\Phi_{-K_f}\,Y_L^{K_i+K_f}(\Omega')\,d\xi\,d\eta\,d\Omega' \,. \qquad \text{V.3}$$

As far as the matrices $B^{Lm}_{\ell j}$ are concerned, quite a number of attempts have been made to calculate these quantities to various degrees of accuracy (53-58). The most useful expression has been obtained by Frӧman (56), and independently, by Nosov (57). Both use a three-dimensional WKB method to arrive at the expression

$$B^{L\,K_i-K_f}_{\ell\,I_f} = (-1)^{\ell\,-K_i+K_f}\,C(I;\,\ell\,I_f;\,K;\,K_f-K_i)\,k^{K_i-K_f}_{\ell L} \,,$$

$$B^{L\,K_i+K}_{\ell\,I_f} = (-1)^{\ell\,+K_i+K_f}\,C(I;\,\ell\,I_f;\,-K_i\;K_f+K_i)\,k^{K_i+K_f}_{\ell L} \qquad \text{V.4}$$

$$k^m_{\ell L} = \int Y^{*m}(\upsilon'\psi'')\,e^{BP_2(\cos\upsilon')}\,Y^m_L(\upsilon'\psi')\,d\cos\upsilon'\;d\psi'$$

B is given in terms of the non-central part of the α-nucleus interaction. Frӧman gives:

$$B = 8.95\ \delta.$$

This estimate is based on the electrostatic interaction with the quadrupole moment alone. The nuclear deformation parameter is defined in accordance with Nilsson (51).

A somewhat superior estimate has been made by Rasmussen (11), who includes also the deformation of the nuclear potential.

He obtains

$$B = 6.18 - 0.045\, Q_0,$$

where $Q_0$ is in barns.

Needless to say in this case the price one pays for simplicity is accuracy. In comparing with methods that are superior in terms of accuracy, one should keep in mind, however, that the nuclear model that plays such a decisive role in the theory is not so accurate as to justify an excessive accuracy in the calculation of the barrier-penetrability matrix.

The final step is to calculate explicitly the $\alpha$-probability amplitudes, by use of the wave functions $\Phi_K$ as given by Equation IV.1.

We discuss first ground-state transitions of even-even nuclei. It is established beyond any doubt that $K_i = K_f = 0$ in these cases and the $\alpha$-probability amplitudes are:

$$G_{LO}(R_0) = \sum_{\Omega_p \Omega_N \Omega_p'} \prod_{\neq \Omega_p} \left(U^i_{\Omega_p'} U^f_{\Omega_p'} + V^i_{\Omega_p'} V^f_{\Omega_p'}\right) \times \prod_{\Omega_N', \neq \Omega_N} \left(U^i_{\Omega_N'} U^f_{\Omega_N'} + V^i_{\Omega_N'} V^f_{\Omega_N'}\right) \times U^f_{\Omega_p} V^i_{\Omega_p} U^f_{\Omega_N} V^i_{\Omega_N} \left[ {}^{\Omega_p - \Omega_p \;\; \Omega_N - \Omega_N}_{LO} \right](R_0), \qquad \text{V.5}$$

where

$$\Gamma_{LM}^{\Omega_1\Omega_2\Omega_3\Omega_4} = R^{3/2} \int A \left(\overset{*}{\psi}_{\Omega_1} \overset{**}{\psi}_{\Omega_2}\right) A \left(\overset{*}{\psi}_{\Omega_3} \overset{*}{\psi}_{\Omega_4}\right) \times \chi_\alpha Y_L^M (\Omega') \, d\xi \, d\Omega' \, .$$

The quantity $\Gamma$ is the contribution to the $\alpha$-amplitude of a specific combination of four Nilsson orbitals, $\Omega_1\Omega_2\Omega_3\Omega_4$, and the $\psi_\Omega$'s are the single-particle wave functions as given by Nilsson. As has been pointed out in the preceding chapter, the form of the BCS wave function implies that protons as well as neutrons are paired up in the initial and final nucleus. (In a spherical nucleus this corresponds to coupling nucleons pairwise to angular momentum zero.) Therefore in the deformed nucleus only combinations of the type $(\Omega,-\Omega)$ must be occupied by a pair of nucleons in the initial nucleus and unoccupied in the final nucleus. The products running over $\Omega'$ finally come from the overlap of the remainder of the wave functions. Their numerical value is usually very close to unity, and in almost all cases they may be disregarded.

The most important feature of Equation V.5 is the averaging process, which suppresses any rapid fluctuation in decay properties that might arise if only one specific combination of orbitals were involved in each decay (11). The averaging process is much more important in this case than it was in the decay of a spherical nucleus. Loosely speaking, one might say that one Nilsson orbit is equivalent to a magnetic substate of a single-particle state with given j. One always averages over magnetic substates in the spherical case, as was pointed out before. In Figs. 2 through 5 calculated results (11, 59) are compared with experimental data (22, 60, 61). Given

are the reduced width $\gamma^2$ of the ground-to-ground transition ($0^+ \rightarrow 0^+$) relative to $Cm^{242}$ and the reduced amplitudes $b_L$ of the transitions to the first and second excited states ( the $2^+$ and $4^+$ states of the ground-state rotational band). A selection from Nilsson's work (51, 52) has been used in the calculation. The general trend of the experimental data is well reproduced by the calculation. Note in particular the small intensity of the transition to the $4^+$ state in Cm. In looking for reasons that could explain the remaining discrepancies one finds that several of the quantities that enter the calculation are uncertain to some extent. These are: The single-particle energies $\epsilon_\Omega$, on which the occupation probabilities depend sensitively; the single-particle wave functions themselves; the residual interaction used in solving the equations of the BCS theory (the residual neutron-proton interaction being neglected completely); and last but not least, the parameters which enter into the calculation of the barrier penetrability, not to speak of the approximations that have been made in solving the barrier penetration problem. In view of these uncertainties the agreement between experiment and theory is rather satisfying. Indeed, these results hold forth the promise that some day such $\alpha$-decay calculations will prove an instrument for resolving details of nuclear structure.

At this point it should also be mentioned that no attempt has yet been made to investigate theoretically $\alpha$-transitions of even-even nuclei other than the ones leading to the ground state rotational band. The experimental data (62) for such transitions are certainly so interesting as to deserve a very thorough theoretical study.

In the decay of odd-mass nuclei, two types of transitions are easily distinguished on the basis of their intensities. Favored transitions have reduced widths comparable to those of their even-even

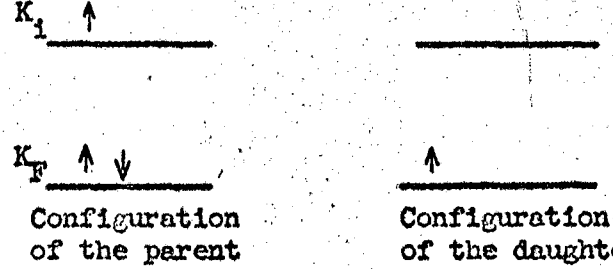
neighbors. Unfavored transitions are hindered by factors of $10^2$ to $10^4$, where these hindrance factors refer to reduced transition rates. It will soon become clear that pairing correlations are largely responsible for this difference. It was recognized very early that favored transitions are characterized by $K_i = K_f$ (63, 64). This implies, on the basis of our model, that the state of the odd nucleon is not changed by the decay process. Indeed the $\alpha$ formation proceeds in the same way as in an even-even nucleus, except that the state of the odd nucleon is blocked for pairs and therefore cannot contribute to the decay. One finds for the amplitude $G_{LO}(R_o)$, in the case of an odd-neutron nucleus (the odd proton case is analogous),

$$G_{LO}(R_o) = \sum_{\substack{\Omega_p \Omega_N \\ \Omega_N \neq K_i}} \overline{\Big|_{\Omega_p' \neq \Omega_p}} \left(U^i_{\Omega_p} U^f_{\Omega_p'} + V^i_{\Omega_p} V^f_{\Omega_p'}\right)$$

$$\times \overline{\Big|_{\Omega_N' \neq \Omega_N}} \left(U^i_{\Omega_N} U^f_{\Omega_N'} + V^i_{\Omega_N} V^f_{\Omega_N'}\right) \qquad \text{V.6}$$

$$\times U^f_{\Omega_p} V^i_{\Omega_p} U^f_{\Omega_N} V^i_{\Omega_N} \Gamma^{\Omega_p - \Omega_p \; \Omega_N - \Omega_N}_{LO}(R_o) \; .$$

The situation is entirely different for an unfavored decay where $K_i = K_f$. Since the odd particle is now in different states initially and finally, there is only one way to form an $\alpha$ particle and a daughter nucleus which has the odd nucleon in the state $K_f$. The $\alpha$ particle must be formed from the odd nucleon of the parent (state $K_i$) and one nucleon from a pair in the state $K_f$. This is schematically illustrated below.



Note that the configuration of the remaining nucleon pairs not shown above must be the same for daughter and parent nuclei.

The calculation yields, for $G_{L\,K_i-K_f}$ ($G_{L\,K_i+K_f}$ is analogous),

$$G_{L\,K_i-K_f}(R_0) = \sum_{\Omega_p} \prod_{\Omega_p' \neq \Omega_p} \left( U^i_{\Omega',p}\, U^f_{\Omega',p} + V^i_{\Omega',p}\, V^f_{\Omega',p} \right) \prod_{\Omega',N \neq K_i,K_f} \left( U^i_{\Omega',N}\, U^f_{\Omega',N} + V^i_{\Omega',N}\, V^f_{\Omega',N} \right) \times U^f_{\Omega_p}\, V^i_{\Omega_p}\, U^f_{K_i}\, V^i_{K_f} \times \Gamma^{\Omega_p-\Omega_p\ \ K_i'-K_f}_{L\ K_i-K_f}(R_0') \quad .$$

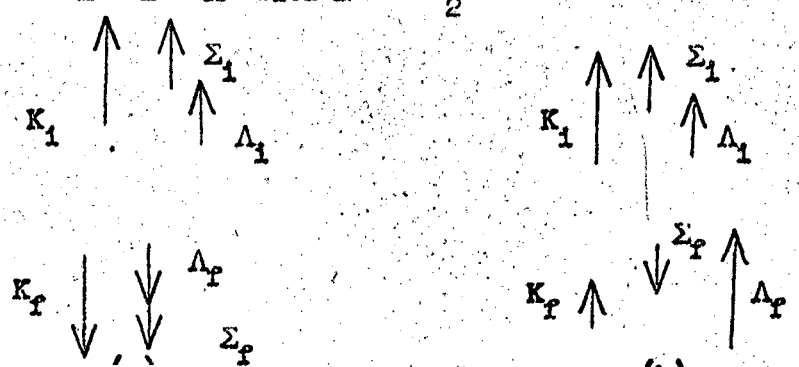
The above formula is significantly different from Equation V.6 which applies to a favored decay: there is no summation over contributions by neutron pairs.(65). It can be shown (11) that all nucleon pairs contribute with positive sign to the amplitude $G_{00}$ ($L = 0$) of a favored decay, and almost all contributions to $G_{20}$ ($L = 2$) are also positive. Consequently the important partial waves of small angular momentum are greatly enhances in a favored transition. This is also true for even-even decays. Since the two lowest partial waves account for about 90 percent of the transition, thier enhancement amounts to a significant enhancement of the total transition. Thus the missing summation over neutron pairs in Equation V.7 explains at least part of the hindrance of an unfavored decay.

Calculated results and the corresponding experimental data (60, 61, 66-69) are presented in Table III. Favored transitions behave very

much like even-even transitions, as was expected. Blocking of a particular state K in most cases results only in an overall reduction of the transition rate. In some cases, however, one partial wave is more strongly affected than others. An example is $Pu^{239}$, where the partial wave of $\ell = 4$ is weakened as compared with the decay of neighboring even-even nuclei. Important information that can be obtained from favored decays is the relative phases of different partial waves. Alpha-gamma correlation experiments (70, 71) and low- temperature nuclear-alignment experiments (72, 73) have shown thet $\ell = 2$ is in phase with $\ell = 0$. Not much is known about the phase of $\ell = 4$. According to the calculation this amplitude changes sign between Cm and Cf (compare Figs. 4 and 5). This sign change should certainly show up in refined measurements.

Besides the general hindrance of unfavored transitions as discussed so far, considerable fluctuations within this class of transitions are observed which are due to the inherent properties of the single-particle states $K_i$ and $K_f$ (74). These fluctuations are faithfully reproduced by the calculation. Moreover, qualitative rules can be established that allow predictions of which unfavored transitions should be more hindered and which less. Since such rules can be helpful in assigning single-particle states in odd-mass nuclei, they will be worked out explicitly. In order to do this let us decompose the projection of the angular momentum K, on the nuclear symmetry axis into its spin $\Sigma$ and orbital part, $\Lambda$.

$$K = \Sigma + \Lambda \quad \text{with} \quad \Sigma = \pm \frac{1}{2}$$



In general $\Lambda$ and $\Sigma$ are not constants of motion because of the presence of a spin-orbit coupling in the single-particle potential. For sufficiently large deformations, however, $\Lambda$ and $\Sigma$ are approximately conserved and one can deduce selection rules that hold approximately. Two cases must be distinguished.

(a) $\Sigma_i$ and $\Sigma_f$ are both parallel or antiparallel to the respective $\Lambda$,

(b) One is parallel and the other one antiparallel to $\Lambda$.

Since the spin function of two like nucleons in the $\alpha$ particle is a singlet spin function, the spins of the nucleons which form the $\alpha$ particle must be anitparallel. Therefore in case (a) the alpha must be formed from nucleons in state $K_i$ and $-K_f$, in case (b) from $K_i$ and $K_f$. This in turn implies that in case (a) the magnetic quantum number m of the $\alpha$ particle equals $K_i - K_f$ at the nuclear surface, whereas in case (b) m is equal to $K_i + K_f$. Thus, in case (a) the angular momentum of the $\alpha$ particle at the nuclear surface is restricted to values equal to or larger than $|K_i - K_f|$, and in case (b), to values equal to or larger than $|K_i + K_f|$. As a consequence one expects that in transitions of type (b) the small angular momenta (between $|K_i - K_f|$ and $K_i + K_f$) will be suppressed, and hence the transition more hindered. The most striking example of such a case is the decay of $Cf^{249}$ to $Cm^{245}$. There are two unfavored transitions to the ground state and first excited state. The initial state is a 9/2-state with $\Lambda = 4$; the final states are a 7/2+ state with $\Lambda = 4$ and a 5/2+ state which has $\Lambda = 2$. The ground-state transition (to the 7/2+ state) is hindered much more than the transition to the 5/2+ state. An example in which these rules can be applied to make level assignments is the decay of $Pu^{239}$. In this decay, two 5/2+ rotational bands are populated: one has $\Lambda = 3$, the

other $\Lambda = 2$. They can be assigned on the basis of the above rules. The assignment in Table III differs from the assignment made by Baranov et al. (69), who studied the $Pu^{239}$ decay experimentally. Cases of special interest are those involving a $K = 1/2$ orbit. Here $|K_i - K_f|$ and $K_i + K_f$ differ only by unity. Two interfering terms are then present in the partial waves of small angular momentum. If the two terms are of the same order of magnitude, this may lead to "alternating intensities", as observed in the decay of $Cm^{243}$ to the ground state rotational band of $Pu^{239}$ (75). Another example is the decay of $Fm^{255}$ that has recently been studied by Asaro et al. (76).

Summarizing one may say that the nuclear shell model including pairing correlations explains satisfactorily the tremendous variations of observed $\alpha$-intensities in the decays of deformed nuclei. That an explanation of such variations required some new idea about $\alpha$-particle formation was already recognized by Perlman and Asaro (77) ten years ago. They concluded a survey of the then existing data by saying: "It seems likely that some of the new ideas when further developed will add appreciably to the explanation of the $\alpha$-decay process, and that the ramifications of these ideas will provide a better understanding of nuclear structure." Apparently we have done a significant step forward towards this goal.

## VI. The Absolute Value of the Decay Constant and the Structure of the Nuclear Surface

The material presented in the preceding chapters certainly justifies a freedom from doubt that the current nuclear models, in particular the various versions of the nuclear shell model, provide a satisfactory description of the $\alpha$-decay process. The only quantity that has so far been omitted from the discussion is the absolute value of the decay constant. It was stated earlier that the calculated value depends sensitively on such nuclear parameters as $R_0$, for example (12). Despite this sensitivity, however, it is difficult to find a reasonable set of parameters giving the correct absolute decay rate. The calculated decay constants always come out too small by a factor between 10 and 1000, depending on what is still considered an acceptable set of parameters and on what $\alpha$-nucleus potential has been used in the calculation.

This rather large discrepancy has led some to the conclusion that the nuclear surface consists mainly of $\alpha$-clusters (76) and that the shell model is therefore incapable of satisfactorily describing the structure of the nuclear surface. Taking this point of view, we find ourselves in the dilemma that on the one hand the shell model cannot describe the cluster structure of the nuclear surface, but on the other hand it predicts correctly the relative amplitudes of various types of $\alpha$ clusters present in the nuclear surface.

Fortunately there seems to be a way out of this dilemma and hope of reconciling the conflicting points of view. In order not to confound the issues let us consider the simplest example, the decay of $Po^{212}$ under the

the assumption that the $Pb^{208}$ core remains unchanged. One can define a "single-particle density" of the outer four nucleons from their wave function $\Psi(1,2,3,4)$,

$$\rho_{s.p.}(R) = \int |\Psi|^2 \sum_{i=1}^{4} \delta(r_i - R)\, d^3r_1\, d^3r_2\, d^3r_3\, d^3r_4\, d\Omega_R \quad .$$

If the four nucleons are each in a definite single-particle state, $\rho_{s.p.}(R)$ takes the simpler form

$$\rho_{s.p.}(R) = \sum_{i=1}^{4} |\phi_i(R)|^2 \quad ,$$

where $\phi_i$ is the radial wave function of nucleon i.

An $\alpha$-particle density can be obtained from the amplitude $g^0_{00}(R)$ of Chapter II:

$$\rho_\alpha(R) = |g^0_{00}(R)|^2 \quad .$$

Note that $J = j = \ell = 0$ in the case under consideration.

In the nuclear surface region ($R > 6.5$ F), where neither $\rho_\alpha$ nor $\rho_{s.p.}$ vanishes (79), the quantity that measures the amount of $\alpha$ clusters is the ratio $\rho_\alpha(R)/\rho_{s.p.}(R)$. Only if this ratio were greater than 0.1 let us say, could one possibly speak of the shell model this ratio ranges from $10^{-6}$ at R = 7.0 F to $10^{-10}$ at R = 9.5 F. Even when $\rho_\alpha$ is multiplied by 1000, a factor which would in any case bring calculated and measured decay constants into agreement, the ratio $\rho_\alpha/\rho_{s.p.}$ remains very much less than unity. One can but conclude that the nuclear surface is

by no means composed entirely of $\alpha$ clusters. There remains the question to be answered: What sort of mechanism could enhance the $\alpha$ amplitude by an amount proportional to the $\alpha$ amplitude as calculated from shell-model wave functions?

It has been pointed out earlier that inclusion of configuration mixing within one major shell increases the $\alpha$-decay rate by a factor of ten in the case of aspherical nucleus in the Pb region (12). What is even more important, the $\alpha$ density $\rho_\alpha$ increases only in the surface region of the nucleus (79). Another important point to note is that the maximum of a $\rho_\alpha(R)$, which is calculated from four definite single-particle functions, moves further and further out when the single-particle functions are taken from higher and higher shells. The possible effect of admixing such higher configurations might be that the $\alpha$ density drops off more slowly than predicted by the shell model. The transition rate would thun increase. At the same time the value of $\rho_\alpha(R)$ [or $g(R)$] somewhere between R = 7.0 F and R = 7.5 F (in the Pb region) would still be given by the shell model with configuration mixing within one major shell. This would leave the relative rates unchanged.

Whether these speculations have any basis in reality can be decided only by further studies. Information about the $\alpha$-nucleus potential $V(R)$ is needed most. A significant amount of the uncertainty about the discrepancy between calculated and measured decay rates must be attributed to insufficient knowledge of this interaction. Unless this interaction is unambiguously determined the shortcomings of the shell model cannot be critically evaluated.

It is clear, however, that there is no need to believe now that the shell model is intrinsically incapable of describing the structure of the nuclear surface as far as the $\alpha$-decay process is concerned.

REFERENCES


1. Hyde, E. K., and G. T. Seaborg, Handbuch der Physik 42 (Springer-Verlag, Berlin, 1957), 205.
2. Everling, F., L. A. König, J. H. E. Mattauch, and A. H. Wapstra, Nucl. Phys. 18, 529 (1960).
3. Rosenblum, S., Compt. Rend. 188, 401 (1929).
4. Gamow, G., Z. Physik 51, 204 (1928).
5. Condon, E. U., and R. W. Gurney, Nature 122, 439 (1928).
6. Thomas, R. G., Progr. Theoret. Phys. (Kyoto) 12, 253 (1928).
7. Wigner, E. P., and L. Eisenbud, Phys. Rev. 72, 29 (1947).
8. Brussaard, P. J., and H. A. Tolhoek, Physica 24, 263 (1958).
9. Mang, H. J., Phys. Rev. 119, 1069 (1960).
10. Harada, K., Progr. Theoret. Phys. (Kyoto) 26, 667 (1961).
11. Mang, H. J., and J. O. Rasmussen, Kgl. Danske Videnskab. Selskab Mat.-Fys. Skr. 2, No. 3 (1962).
12. Zeh, H. D., and H. J. Mang, Nucl. Phys. 29, 529 (1962).
13. Perlman, I., and J. O. Rasmussen, chapter on "Alpha Radioactivity" in Handbuch der Physik, 42 (Springer-Verlag, Berlin, 1957) 109.
14. Flamm, E., and F. Asaro, Phys. Rev. 129, 290 (1963) and the references quoted there.
15. Zeh, H. D., Z. Phys. 175, 490 (1963).
16. Fock, V., J. Phys. U.S.S.R. 11, 112 (1947).
17. Petzold, J., Z. Phys. 155, 422 (1959).
18. Morse, P. M. and H. Feshbach, Methods of Theoretical Physics (McGraw-Hill Book Co., Inc., New York, 1953).
19. Hofstaedter, R., Rev. Mod. Phys. 28, 214 (1956).

20. Belyaev, B. N., A. V. Kalyamin, A. N. Murin, Bull. Acad. Sci. U.S.S.R. (English Transl.) 25, 886 (1961).

21. Igo, G., Phys. Rev. 115, 1665 (1959).

22. Rasmussen, J. O., Phys. Rev. 113, 1593 (1959).

23. True, W. W., and K. W. Ford, Phys. Rev. 109, 1675 (1958).

24. Kearsley, M. J., Nucl. Phys. 4, 151 (1957).

25. Blomquist, J. and S. Wahlborn, Arkiv Fysik 16, 545 (1960).

26. Gorodetzky, S., A. Gallmann, A. C. Knipper, and R. Armbruster, Compt. Rend. 237, 245 (1953).

27. Jentschke, W., A. C. Juveland, and G. H. Kinsey, Phys. Rev. 96, 231 (1954).

28. Singes, S., Thesis, University of Illinois, 1957 (unpublished).

29. Gorodetzky, S., Beck, Knipper, Manquenouille, and Richert, Compt. Rend. 254, 2319 (1962).

30. Walen, R. J., and G. Bastin Scoffier, J. Phys. Radium 20, 589 (1959).

31. Walen, R. J., and G. Bastin Scoffier, Compt. Rend. 245, 676 (1957).

32. Walen, R. J., and G. Bastin Scoffier, Nucl. Phys. 16, 246 (1960).

33. Golonetskii, V. S., L. I. Rusinov, and Y. I. Filimonov, Soviet Phys. JETP 10, 395 (1960).

34. Rusinov, L. I., Y. N. Andreev, V. S. Golonetskii, M. I. Kislov, and Y. I. Filimonov, Soviet Phys. JETP 13, 707 (1961).

35. Perlman, I., F. Asaro, A. Ghiorso, A. Larsh, and R. Latimer, Phys. Rev. 127, 917 (1962).

36. Glendenning, N. K., Phys. Rev. 127, 923 (1962).

37. Karnaukhov, V. A., Soviet Phys. JETP 15, 671 (1962).

38. Bardeen, J., L. N. Cooper, and J. R. Schrieffer, Phys. Rev. 108, 1115 (1957).

39. Bogoliubov, N. N., Soviet Phys. JETP 34, 41 (1958).

40. Bohr, A., B. R. Mottelson, and D. Pines, Phys. Rev. 110, 936 (1958).

41. Beliaev, S. T., Kgl. Danske Videnskab. Selskab Mat.-Fys. Medd. 31, No. 11 (1958).

42. Soloviev, V. G., Nucl. Phys. 9, 655 (1959).

43. Kisslinger, L. S., and R. A. Sorensen, Kgl. Danske Videnskab. Selskab Mat.-Fys. Medd. 32, No. 8 (1961).

44. Nilsson, S. G., O. Prior, Kgl. Danske Videnskab. Selskab Mat.-Fys. Medd. 32, No. 16 (1961).

45. Macfarlane, R. P., J. O. Rasmussen and M. Rho, Phys. Rev. (to be published).

46. Toth, K. S., and J. O. Rasmussen, Nucl. Phys. 16, 474 (1960).

47. Toth, K. S., and J. O. Rasmussen, Phys. Rev. 109, 121 (1958).

48. Riezler, W., and G. Kauw, Z. Naturforsch. 14a, 196 (1959).

49. Goeppert-Mayer, M., and J. H. D. Jensen, Elementary Theory of Nuclear Shell Structure, (John Wiley and Sons, New York, 1955).

50. Bohr, A., and B. R. Mottelson, Kgl. Danske Videnskab. Selskab Mat.-Fys. Medd. 27, No. 16 (1953).

51. Nilsson, S. G., Kgl. Danske Videnskab. Selskab Mat.-Fys. Medd. 29, No. 16 (1955).

52. Mottelson, B. R., and S. G. Nilsson, Kgl. Danske Videnskab. Selskab Mat.-Fys. Skr. 1, No. 8 (1959).

53. Pennington, E. M., and M. A. Preston, Can. J. Phys. 36, 944 (1958).

54. Rasmussen, J. O., and E. R. Hansen, Phys. Rev. 109, 1656 (1958).

55. Chasman, R. and J. O. Rasmussen, Phys. Rev. 112, 512 (1958).

56. Frŏman, P. O., Kgl. Danske Videnskab. Selskab Mat.-Fys. Skr. 1, No. 3 (1957).

57. Nosov, V. G., Soviet Phys. JETP 10, 631 (1960).

58. Strutinskii, V. M., Soviet Phys. JETP 5, 1150 (1957).

59. Mang, H. J., J. K. Poggenburg, and J. O. Rasmussen, Bull. Am. Phys. Soc. 8, 315 (1963).

60. Hyde, E. K., I. Perlman, and G. T. Seaborg, The Nuclear Properties of the Heavy Elements, Vol. I, Systematics of Nuclear Structure and Radioactivity, (Prentice-Hall, Inc., Englewood Cliffs, New Jersey, 1964).

61. Strominger, D., J. Hollander, and G. T. Seaborg, Rev. Mod. Phys. 30, 585 (1958).

62. Bjørnholm, S., M. Lederer, F. Asaro, and I. Perlman, Phys. Rev. 130, 2000 (1963).

63. Perlman, I., A. Ghiorso, and G. T. Seaborg, Phys. Rev. 77, 26 (1950).

64. Bohr, A., P. O. Frӧman, and B. R. Mottelson, Kgl. Danske Videnskab. Selskab Mat.-Fys. Medd. 29, No. 10 (1955).

65. Soloviev, V. G., Phys. Letters 1, 202 (1962).

66. Rasmussen, J. O., Phys. Rev. 115, 1675 (1959).

67. Baranov, S. A., V. M. Kulakov, P. S. Samoilov, A. G. Zelenkov, Yu. F. Rodionov, and S. V. Pirozhkov, Soviet Phys. JETP 14, 1053 (1962).

68. Novikova, G. J., L. N. Kondrat'ev, Iu. P. Sobolev, and L. L. Gold'in, Soviet Phys. JETP, 5, 832 (1957).

69. Baranov, S. A., V. M. Kulakov, and S. N. Belenky, Nucl. Phys. 41, 95 (1963).

70. Krohn, V. E., T. B. Novey, and S. Raboy, Phys. Rev. 105, 234 (1957).

71. Siegbahn, K., and F. Asaro, Phys. Letters 2, 323 (1962).

72. Navarro, Q. O., J. O. Rasmussen, and D. A. Shirley, Phys. Letters 2, 353 (1962).

73. Hanauer, S. H., J. W. T. Dabbs, L. D. Toberts, and G. W. Parker, Phys. Rev. 124, 1512 (1961).

74. Prior, O., Arkiv Fysik 16, 15 (1959).

75. Asaro, F., S. G. Thompson, F. S. Stephens, and I. Perlman, Bull. Am. PAm. Phys. Soc. 2 393 (1957).

76. Asaro, F., S. Bjornholm, and I. Perlman, Phys. Rev. 133, B291 (1964).

77. Perlman, I. and F. Asaro, Ann. Rev. Nucl. Sci. 4, 187 (1954).

78. Wilkinson, D. H., in Proceedings of the Rutherford Jubilee International Conference, Manchester 1961.

79. Harada, K., Progr. Theoret. Phys. (Kyoto) 27, 430 (1962).

Table I. Single-particle states in the lead region.

| $Bi^{209}$ proton states | Excitation energy MeV | $Pb^{209}$ neutron states | Excitation energy MeV |
|---|---|---|---|
| $3P_{1/2}$ | — | $3d_{3/2}$ | 2.52 |
| $3P_{3/2}$ | — | $2g_{7/2}$ | 2.47 |
| $2f_{5/2}$ | — | $4s_{1/2}$ | 2.03 |
| $1i_{13/2}$ | 1.60 | $1j_{15/2}$ | 1.56 |
| $2f_{7/2}$ | 0.90 | $1i_{11/2}$ | 0.77 |
| $1h_{9/2}$ | 0.00 | $2g_{9/2}$ | 0.00 |
| **$Tl^{207}$ proton hole states** | | **$Pb^{207}$ Neutron hole states** | |
| $3s_{1/2}$ | 0.00 | $3P_{1/2}$ | 0.00 |
| $2d_{3/2}$ | 0.35 | $2f_{5/2}$ | 0.57 |
| $1h_{11/2}$ | — | $3P_{3/2}$ | 0.89 |
| $2d_{5/2}$ | — | $1i_{13/2}$ | 1.64 |
| $1g_{7/2}$ | — | $2f_{7/2}$ | 2.34 |
| | | $1h_{9/2}$ | 3.41 |

Table II. Decay amplitudes of $Po^{210}$, $Po^{211}$, $Bi^{211}$, and $Po^{212}$, calculated and experimental.
I(j) = Intensity of the transition to the level j in the daughter nucleus.
A(j,ℓ) = Amplitude of the ℓth partial wave of the transition to the level j.

| | | One-body model | Shell-model harmonic oscillator | Shell model Woods-Saxon potential | Shell model with configuration mixing (Woods-Saxon potential) | Experimental values |
|---|---|---|---|---|---|---|
| | $T_{1/2}(Po^{210})$ | | | | | 138d |
| | $T_{1/2}(Po^{211})$ | 0.19 sec | 0.18 sec | 0.14 sec | 0.44 sec | 0.52 sec |
| | $T_{1/2}(Po^{212})$ | | | | $4.75\times10^{-7}$ sec | $3.04\times10^{-7}$ sec |
| | $T_{1/2}(Bi^{211})$ | 6.85 min | 18.4 min | 21 min | 2.56 min | 2.2 min |
| | I(5/2)/(1/2) | $6.85\times10^{-2}$ | $1.20\times10^{-2}$ | $0.80\times10^{-2}$ | $0.79\times10^{-2}$ | $0.53\times10^{-2}$ |
| | I(3/2)/(1/2) | $0.46\times10^{-2}$ | $0.53\times10^{-2}$ | $0.49\times10^{-2}$ | $0.47\times10^{-2}$ | $0.50\times10^{-2}$ |
| $Po^{211}$ | A(5/2,5)/A(5/2,3) | 0.48 | -0.90 | -0.90 | -0.90 | -0.96 |
| | A(5/2,7)/A(5/2,3) | 0.16 | 0.60 | 0.60 | 0.61 | 0.55 |
| | A(3/2,5)/A(3/2,3) | 0.47 | -0.35 | -0.35 | -0.35 | -0.14<br>-0.35[a] |
| $Bi^{211}$ | I(3/2)/I(1/2) | .25 | .18 | .14 | .15 | .19 |
| | A(3/2,5)/A(3/2,3) | 0.47 | -0.35 | -0.35 | -0.35 | -0.27 |
| $Po^{210}$ | I(2)/I(0) | $.8\times10^{-5}$ | $2.9\times10^{-5}$ | $1.4\times10^{-5}$ | $1.4\times10^{-5}$ | $1.2\times10^{-5}$ |

[a] If the transition $P_{3/2}\rightarrow P_{1/2}$ is assumed to be pure M1 one obtains the value -0.14 from the measured angular correlation. An 1.2 percent admixture of E2 gives the value -0.35 (12).



UCRL-11326

Table III. Decay rates of odd mass deformed nuclei relative to the $Cm^{242}$ ground state transition (only a representative sample of data is given).

| Parent nucleus | Initial Nilsson state | Final Nilsson state | Angular momentum of the daughter nucleus | Excitation energy of the daughter nucleus (kev) | Reduced transition rate Calculated | Reduced transition rate Experimental | Remarks |
|---|---|---|---|---|---|---|---|
| $Np^{237}$ | 5/2+[642] | 5/2+[642] | 5/2 | 86.0 | 861.0 | 236.0 | No Coriolis mixing between the 5/2+[642] band and the 3/2+[651] band has been taken into account |
| | | | 7/2 | 105.0 | 219.5 | 178.8 | |
| | 5/2+[642] | 1/2-[530] | 1/2 | 6.0 | .434 | 1.20 | |
| | | | 3/2 | 0.0 | 1.825 | 3.43 | |
| | | | 5/2 | 69.0 | 3.245 | 5.16 | |
| | | | 7/2 | 57.0 | 33.505 | 3.90 | |
| $Pu^{239}$ | 1/2+[631] | 1/2+[631] | 1/2 | .07 | 386.0 | 379.0 | |
| | | | 3/2 | 13.5 | 79.3 | 94.5 | |
| | | | 5/2 | 51.7 | 119.0 | 126.7 | |
| | | | 7/2 | 84.0 | 2.48 | 0.657 | |
| | | | 9/2 | 151.0 | 3.11 | 0.620 | |
| | 1/2+[631] | 5/2+[622] | 5/2 | 129.0 | 0.062 | 0.181 | The assignment made is certain only in so far that the weaker transitions must go to the 5/2+[622] band and not to the 5/2+[633] band. |
| | | | 7/2 | 172.0 | 0.221 | 0.347 | |
| | | | 9/2 | 224.0 | 0.240 | 0.442 | |
| | 1/2+[631] | 5/2+[633] | 5/2 | 333.0 | 2.355 | 2.97 | |
| | 1/2+[631] | 5/2+[633] | 5/2 | 426.0 | 2.355 | 3.30 | This assignment is also possible on the basis of the α intensities |
| | | | 7/2 | 470.0 | 1.100 | 2.50 | |
| | | | 9/2 | 530.0 | 4.690 | 3.20 | |
| $Am^{241}$ | 5/2-[523] | 5/2-[523] | 5/2 | 59.57 | 611.0 | 697.8 | |
| | | | 7/2 | 103.0 | 164.0 | 201.7 | |
| | | | 9/2 | 158.6 | 60.9 | 43.7 | |
| | | | 11/2 | 225.0 | 3.69 | 1.16 | |
| | | | 13/2 | 307.0 | 1.36 | 0.61 | |
| | 5/2-[523] | 5/2+[642] | 5/2 | 0.0 | 0.496 | 0.940 | |
| | | | 7/2 | 33.2 | 0.332 | 0.694 | |
| | | | 9/2 | 76.5 | 0.154 | 0.415 | |
| | | | 11/2 | 127.0 | 0.051 | 0.192 | |

(continued)

Table III. (Continued)

| | | | | | | | |
|---|---|---|---|---|---|---|---|
| | 5/2-[523] | 1/2-[530] | 1/2 | --- | 0.002 | --- | The transition is not observed. It is difficult to assign other observed levels on the basis of α-intensities alone to this rotational band to the 1/2- state. |
| | | | 3/2 | 270 | 0.162 | 0.073 | |
| $Am^{243}$ | 5/2-[523] | 5/2-[523] | 5/2 | 74.0 | 503.0 | 772.6 | |
| | | | 7/2 | 117.0 | 130.5 | 175.2 | |
| | | | 9/2 | 173.0 | 48.0 | 44.3 | |
| | 5/2-[523] | 5/2+[642] | 5/2 | 0.0 | 0.355 | 0.502 | |
| | | | 7/2 | 31.0 | 0.252 | 0.731 | |
| $Cm^{243}$ | 5/2+[622] | 5/2+[622] | 5/2 | 285.5 | 458.0 | 456.4 | |
| | | | 7/2 | 330.0 | 117.3 | 125.3 | |
| | | | 9/2 | 387.9 | 42.6 | 35.7 | |
| | 5/2+[622] | 1/2+[631] | 1/2 | 0.0 | 0.056 | 0.209 | |
| | | | 3/2 | 7.85 | 0.351 | 1.134 | |
| | | | 5/2 | 57.30 | 0.264 | 0.363 | |
| | | | 7/2 | 75.71 | 0.775 | 2.996 | |
| | | | 9/2 | 163.69 | 0.228 | 0.142 | |
| | | | 11/2 | 193.10 | 0.380 | 0.999 | |
| | 5/2+[622] | 7/2-[743] | 7/2 | 391.60 | 1.45 | 4.700 | |
| | | | 9/2 | 434.15 | 1.01 | 6.078 | |
| | | | 11/2 | 485.00 | 0.566 | 3.912 | |
| $Cf^{249}$ | 9/2-[734] | 9/2-[734] | 9/2 | 394 | 333.4 | 286.6 | |
| | | | 11/2 | 450 | 43.8 | 31.2 | |
| | | | 13/2 | 511 | 9.05 | 6.36 | |
| | 9/2-[734] | 7/2+[624] | 7/2 | 0.0 | 0.166 | 0.059 | |
| | | | 9/2 | 56.0 | 0.129 | 0.065 | |
| | | | 11/2 | 124.0 | 0.073 | 0.052 | |
| | | | 13/2 | 207.0 | 0.024 | 0.028 | |
| | 9/2-[734] | 5/2+[622] | 5/2 | 257.0 | 0.545 | 2.079 | |
| | | | 7/2 | 301.0 | 0.748 | 3.210 | |
| | | | 9/2 | 357.0 | 0.546 | 2.590 | |
| | | | 11/2 | 422.0 | 0.263 | 2.440 | |
| $Es^{253}$ | 7/2 [633] | 7/2 [633] | 7/2 | 0 | 271.1 | 375.3 | |
| | | | 9/2 | 41.7 | 31.4 | 49.3 | |
| | | | 11/2 | 93.4 | 8.69 | 7.83 | |
| | | | 13/2 | 156.0 | .490 | 1.72 | |
| $Fm^{255}$ | 7/2+[613] | 1/2+[620] | 1/2 | 0 | .082 | .162 | |
| | | | 3/2 | 25 | .133 | .220 | |
| | | | 5/2 | 48 | .541 | 1.180 | |
| | | | 7/2 | 106 | --- | --- | This transition is masked by the favored transition. |
| | | | 9/2 | 149 | .335 | .795 | |

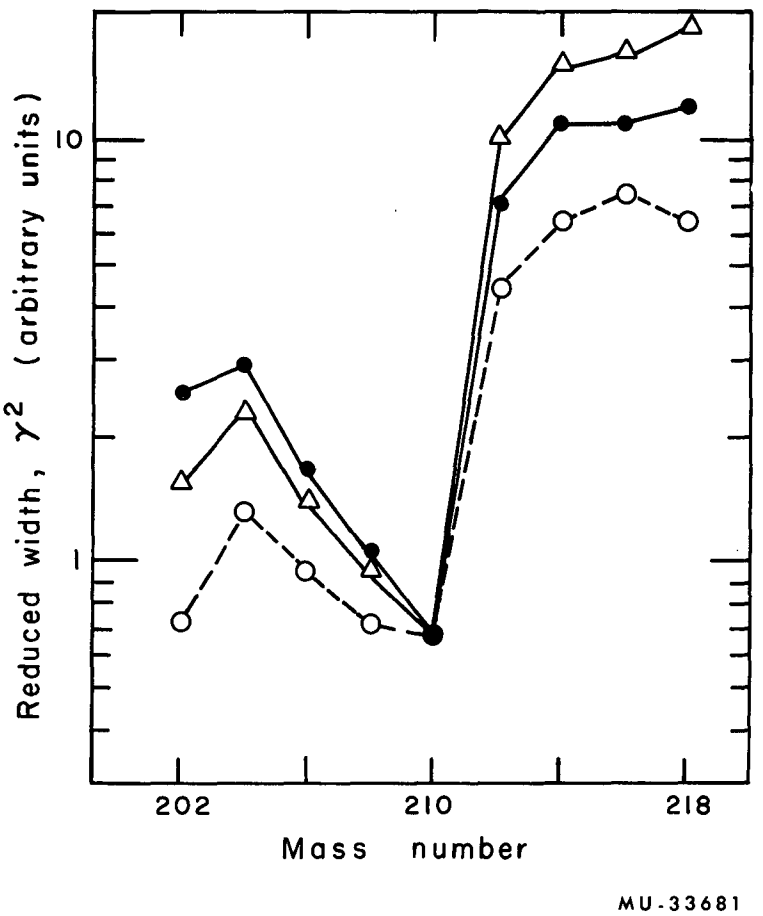



Fig. 1. Reduced widths $\gamma^2$ of even-even polonium isotopes (in arbitrary units) given as a function of mass number. —●—, computed from measured decay constants with the help of Igo's optical-model potential (22); —△—, also computed from measured decay constants, but a pure Coulomb potential has been used with a cutoff at 9.3 F (13); --O-- calculated from the shell model (9).

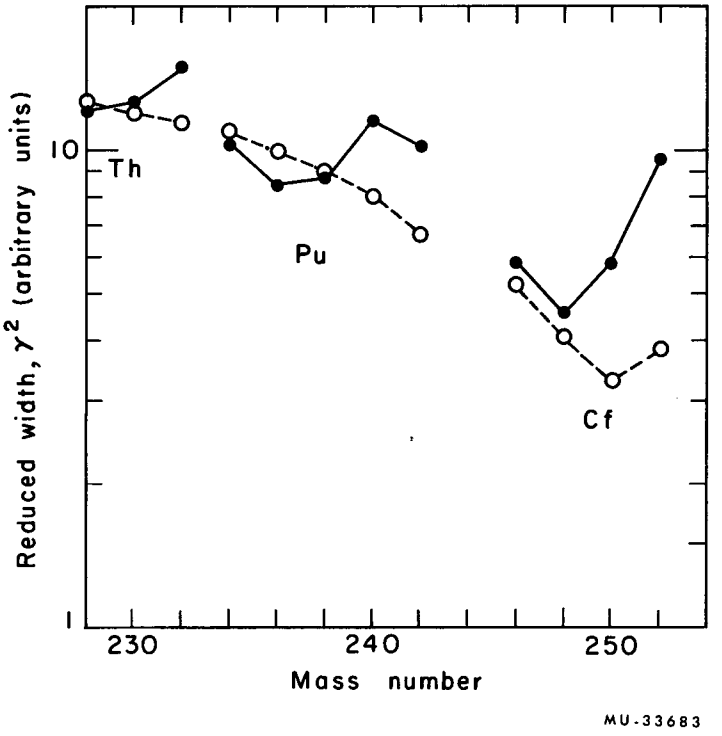



Fig. 2. Reduced widths of the ground-state transitions of even isotopes of U, Cm, and Fm. O, calculated; ●, experimental. The real part of the optical-model potential has been used as α-nucleus interaction. Calculated points are normalized at $Cm^{242}$.

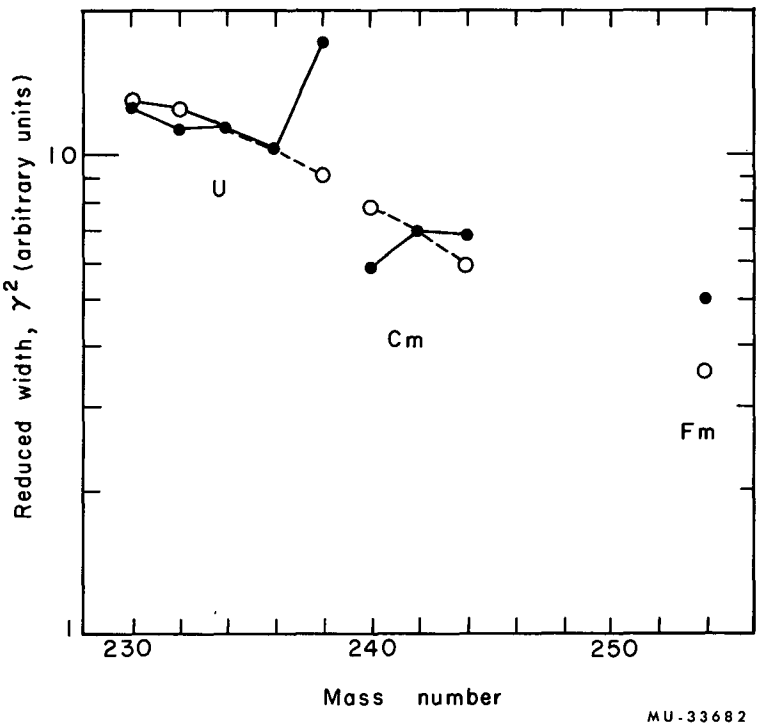



Fig. 3. Reduced widths of the ground-state transitions of even isotopes of Th, Pu, and Cf. O, calculated; ●, experimental. The real part of the optical-model potential has been used as $\alpha$-nucleus interaction. Calculated points are normalized at $Cm^{242}$.

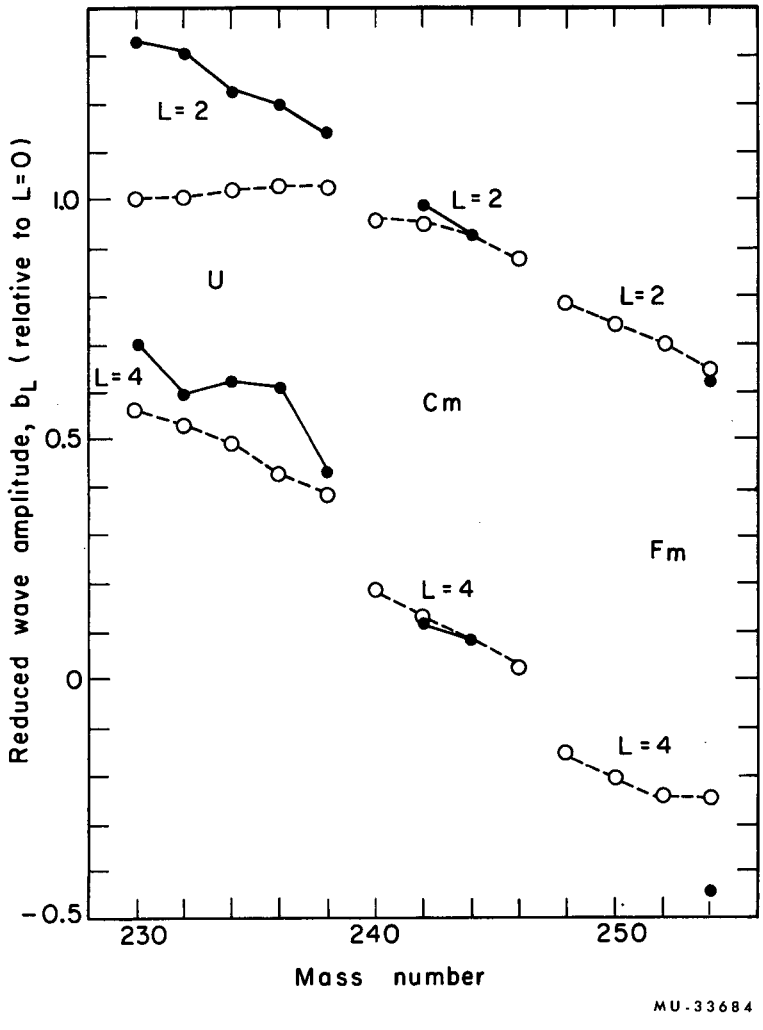



Fig. 4. Reduced wave amplitudes of transitions to the $2^+$ and $4^+$ states of the ground-state rotational band. O, calculated; ●, experimental.

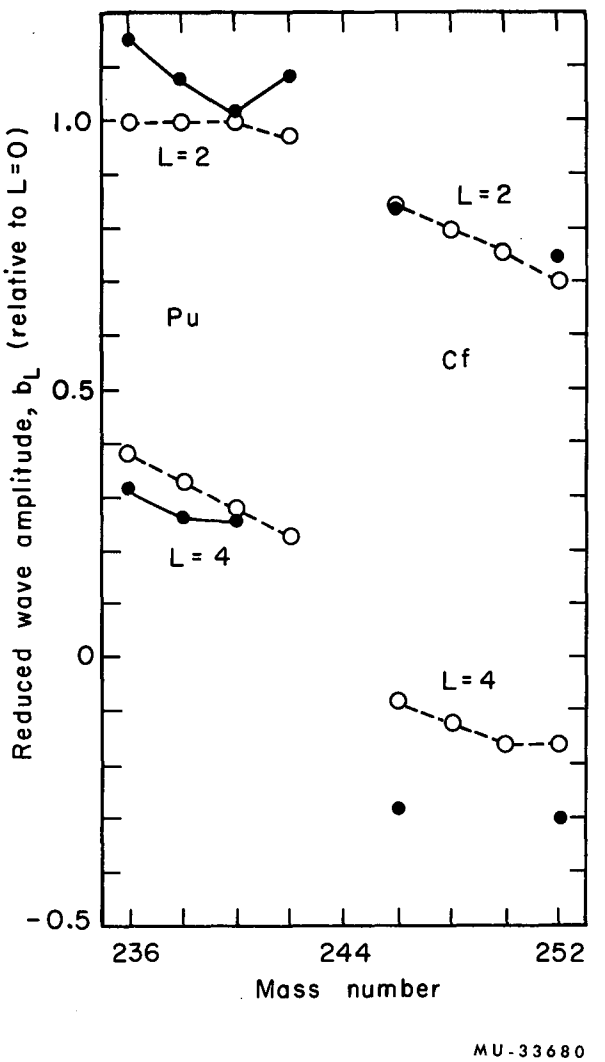



Fig. 5. Reduced wave amplitudes of transitions to the $2^+$ and $4^+$ states of the ground-state rotational band. O, calculated; ●, experimental.

This report was prepared as an account of Government sponsored work. Neither the United States, nor the Commission, nor any person acting on behalf of the Commission:

A. Makes any warranty or representation, expressed or implied, with respect to the accuracy, completeness, or usefulness of the information contained in this report, or that the use of any information, apparatus, method, or process disclosed in this report may not infringe privately owned rights; or

B. Assumes any liabilities with respect to the use of, or for damages resulting from the use of any information, apparatus, method, or process disclosed in this report.

As used in the above, "person acting on behalf of the Commission" includes any employee or contractor of the Commission, or employee of such contractor, to the extent that such employee or contractor of the Commission, or employee of such contractor prepares, disseminates, or provides access to, any information pursuant to his employment or contract with the Commission, or his employment with such contractor.

